Columnar defect formation in nanorod/$Tl_2Ba_2Ca_2Cu_3O_z$ superconducting composites

Peidong Yang and Charles M. Lieber[a)]
Department of Chemistry and Division of Applied Sciences, Harvard University, Cambridge, Massachusetts 02138

(Received 24 February 1997; accepted for publication 9 April 1997)

Nanorod/superconductor composites were formed by depositing $Tl_2Ba_2Ca_2Cu_3O_z$ (Tl-2223) thick films on high density MgO nanorod arrays that were grown on MgO single crystal substrates. Electron microscopy studies show that this approach creates a high density of columnar defects normal to the CuO_2 planes within crystal grains of the composites. The nanorod/superconductor composites exhibited enhanced critical current densities and an upward shift in the irreversibility line compared with reference samples. These results demonstrate that a nanorod-composite approach represents an effective strategy for introducing correlated defects into high-T_c superconductors, and thus may be useful for applications. © *1997 American Institute of Physics.* [S0003-6951(97)02723-X]

Thermally activated flux flow (TAFF) represents an important intrinsic limitation to the realization of large critical current density (J_c) high-temperature superconductor (HTS) applications.[1] Although significant effort has been placed on high-J_c $Bi_2Sr_2Ca_{n-1}Cu_nO_z$ ($n=2,3$) and $YBa_2Cu_3O_z$ wires,[2,3] thallium based materials, such as $Tl_2Ba_2Ca_2Cu_3O_z$ (Tl-2223), are also promising candidates for large scale applications since they combine high T_cs with a platelike morphology that can produce good intergranular contacts. However, the problem of TAFF still limits J_c in the technologically important high temperature and field regime.

Theoretical[4] and experimental[5,6] studies have shown that nanometer diameter columnar defects can reduce the problem of TAFF. The interaction of flux lines with columnar defects results in a large pinning energy that effectively resists thermally activated motion, and thus increases J_c significantly at high temperatures and fields. Columnar defects can be created by irradiating samples with heavy ions having energies on the order of a GeV. This approach is of limited use for large-scale applications, since the heavy ions have a short penetration depth and the resulting defects have a low thermal stability.[7] High-energy (0.8 GeV) protons have also been used to create isotropic columnar defects in BSCCO materials through fission of the Bi nuclei.[8] An advantage of this latter approach is the large, 0.5 m penetration depth of the protons that enables the creation of columnar defects in completed wires; however, it remains unclear whether high-energy, ion-irradiation techniques will be economically viable for large-scale commercial applications. Hence, we have been developing a chemical approach to create columnar defects in HTS that involves (1) the growth of inert oxide whiskers with nanometer scale diameters (nanorods) and (2) subsequent incorporation of these nanorods into a HTS matrix.[9] In this letter, we report the first studies of the growth, structure, and critical currents for MgO nanorod/Tl-2223 composite materials.

The MgO nanorods used to make the HTS composites were grown as arrays on the (001) surfaces of single crystal MgO substrates using a vapor–solid process.[9,10] Scanning electron microscopy (SEM) images of a typical MgO nanorod array [Fig. 1(a)] show that the nanorods grow primarily perpendicular to the substrate along the ⟨001⟩ direction. The density of nanorods in Fig. 1(a) is about 2×10^9 cm^{-2}, although densities as high as 2×10^{10} cm^{-2} can be obtained using this procedure. In addition, transmission electron microscopy (TEM) studies of nanorods removed from the sub-

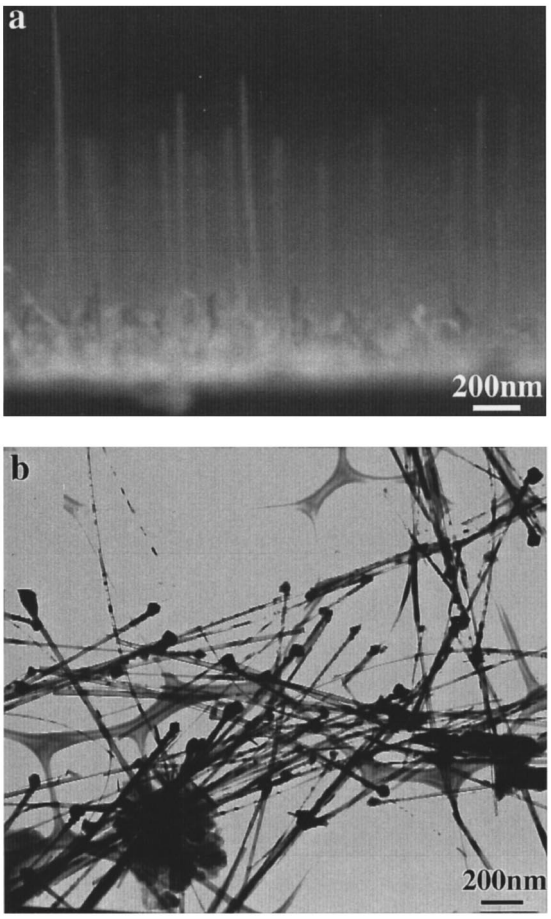

FIG. 1. (a) SEM micrograph of a MgO nanorod array grown on MgO single crystal substrate. The areal density of nanorods is approximately 2×10^9 cm^{-2}. (b) TEM micrograph of MgO nanorods cleaved from the substrate surface in (a).

[a)]Electronic mail: cml@cmliris.harvard.edu

 0003-6951/97/70(23)/3158/3/$10.00

strate show that the nanorods have diameters ranging from 4 to 40 nm with an average of 15 nm and typical lengths of 1–3 μm [Fig. 1(b)]. These dimensions are ideally suited for pinning magnetic flux lines in the HTS.

Textured thick films of Tl-2223 were prepared on (001) single crystal MgO substrates with and without MgO nanorod arrays by a two-stage process. First, pulsed laser deposition (PLD) at 200 °C was used to prepare an amorphous, 1–2 μm thick film of $Ba_2Ca_2Cu_3O_z$. Second, this amorphous material was annealed *ex situ* to incorporate thallium and texture the film.[11] During the thallination, the amorphous films are encapsulated with small amount of Tl-2223 powder in Ag foils and put at one end of the half-sealed alumina tube with Tl_2O_3 at the other end. The Tl source temperature was kept at 890 °C while the temperature of the films was maintained at 790 °C. X-ray diffraction θ–2θ scans made on annealed thick films show that nanorod/Tl-2223 composites and Tl-2223 reference samples are well textured with the *c* axis normal to the substrate surface. In addition, these data indicate that the samples are ~95% Tl-2223 phase with ~5% Tl-2212 impurity [Fig. 2(a)]. The T_cs of the composite and reference samples determined magnetically were both 120 K; that is, no degradation of T_c was observed in the nanorod/HTS composites.

We have also examined the microstructure of the nanorod composites at the different stages of preparation. A cross-sectional SEM image of a nanorod array after low-temperature PLD shows that the nanorod forest is filled with amorphous $Ba_2Ca_2Cu_3O_z$ and that many rods protrude from the amorphous matrix [Fig. 2(b)]. After thallination and texturing, the superconducting composite films have a smooth platelike morphology with a high density of nanorods protruding from the basal *ab* plane of the Tl-2223 crystal grains [Fig. 2(c)]. The areal density $\sim 1\times 10^9$ cm^{-2} corresponds quite well with the nanorod density determined before the formation of this specific sample. In addition, TEM and spatially resolved energy-dispersive x-ray fluorescence measurements confirmed that the MgO nanorods (1) create oriented columnar defects inside crystal grains, (2) are oriented along the *c* axis, and (3) form a compositionally sharp interface with the Tl-2223 superconductor matrix.

We characterized J_c for the nanorod/Tl-2223 composites and Tl-2223 reference samples through measurements of the sample magnetization *M* as a function of field and temperature. The sample $J_c(H,T)$ is related to the hysteresis in magnetization, $\Delta M(H,T)$, by a geometric factor, assuming that supercurrents flow within the entire sample: $J_c = 15\Delta M/R$, where *R* is the radius of the entire sample.[12] Although this approach could underemphasize grain boundary limitations on J_c, it is appropriate for probing the intrinsic effect of defect pinning within crystal grains that is the focus of our studies. The field dependence of J_c determined at several temperatures for reference and composite samples is shown in Fig. 3(a); these results are typical for the composite and reference samples. In general, the nanorod/Tl-2223 composites exhibit large increases in J_c compared with the reference samples, and these increases are especially significant at the higher field and temperature regime of our measurements. The large increases in J_c are attributed to enhanced vortex pinning by the nanorod columnar defects. The

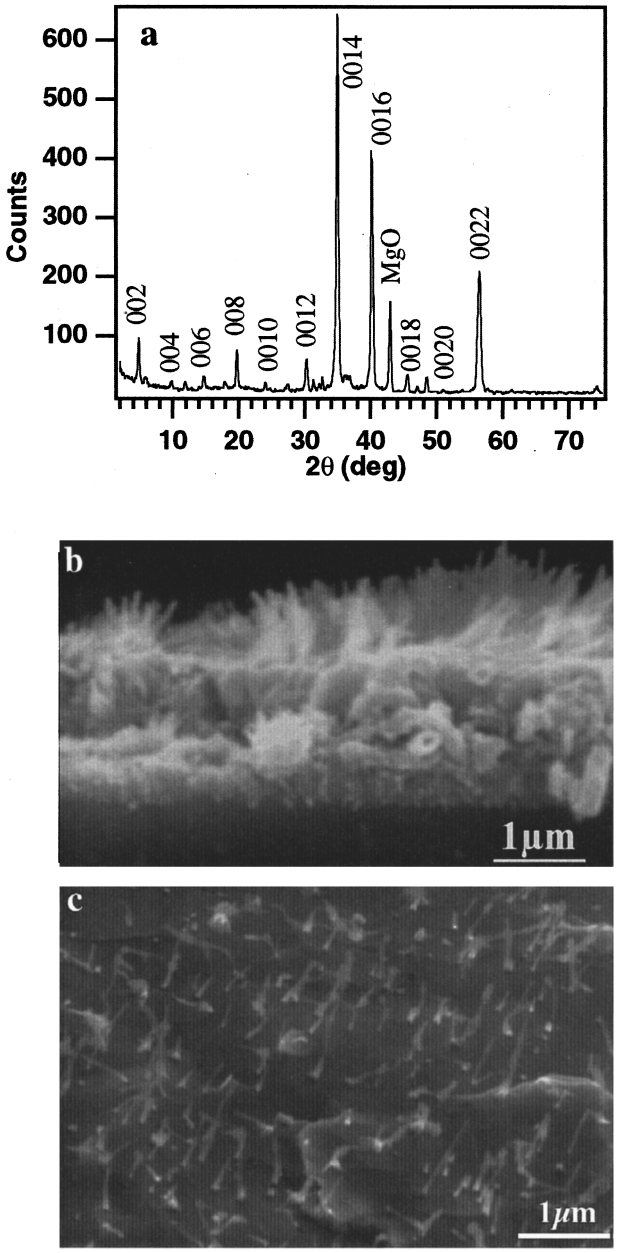

FIG. 2. (a) X-ray diffraction pattern of a nanorod/Tl-2223 composite obtained after *ex situ* annealing. (b) Cross-sectional SEM image of the nanorod array after deposition of the amorphous $Ba_2Ca_2Cu_3O_z$. (c) SEM image of the annealed composite surface recorded at a 45° angle. The light, rodlike structures protruding from the darker Tl-2223 surface correspond to the MgO nanorods.

results at elevated field and temperature are characteristic of the behavior expected for pinning by correlated defects and cannot be explained by point-defect pinning.

We have also examined the temperature dependence of J_c for selected fields to show clearly changes in pinning at elevated temperatures. Results obtained on nanorod/Tl-2223 composites and reference samples at $H=0.5$ and 0.8 T are shown in Fig. 3(b). In the reference samples, J_c fell off rapidly with temperature as a result of TAFF, while in the nanorod/Tl-2223 composites, this fall-off was reduced significantly and led to order of magnitude improvements in J_c above 40 K. The large increases in $J_c(H,T)$ for the nanorod/Tl-2223 composites can also be summarized by a

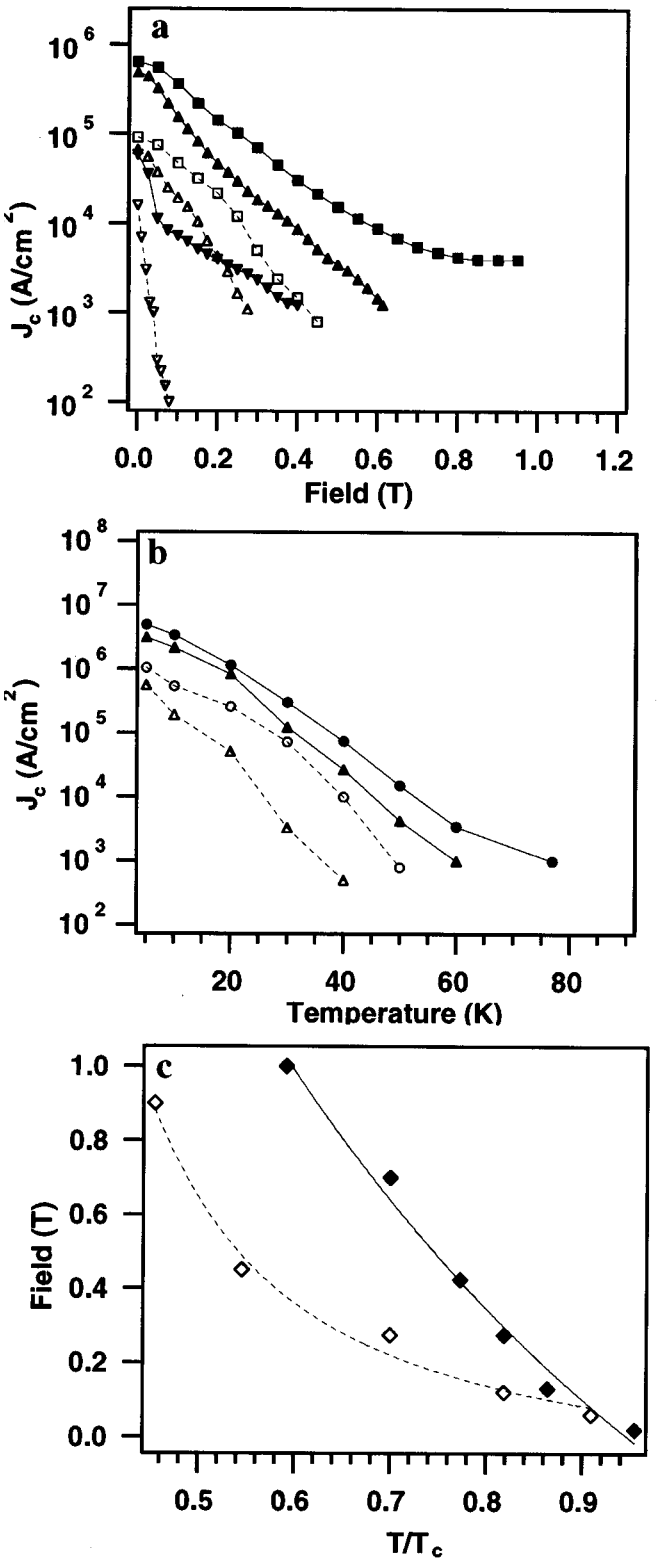

FIG. 3. (a) Comparison of the field dependence of J_c for Tl-2223/nanorod composite and Tl-2223 reference samples. The squares, triangles, and inverted triangles correspond to temperatures of 50, 60, and 90 K, respectively. (b) Comparison of the temperature dependence of J_c in typical Tl-2223/nanorod composite and reference samples at 0.5 and 0.8 T. The circles and triangles correspond to fields of 0.5 and 0.8 T, respectively. (c) Plot of the irreversibility line for Tl-2223/nanorod composite and reference samples. Solid lines and filled symbols correspond to the nanorod composite samples, while dashed lines and open symbols correspond to reference samples. The lines in (a), (b), and (c) are guides to the eye.

plot of the irreversibility line in the $H=T$ plane [Fig. 3(c)]. The irreversibility point was taken as the field at which the hysteresis loop closed for each temperature. For our experiments, the closing criterion was taken to be 5×10^{-6} emuand was applied to similar-sized composite and reference samples in the analysis. Significantly, we find large upward shifts in the irreversibility line for the nanorod/Tl-2223 composites; for example, at 0.5 and 1.0 T the shifts are 30 and 35 K, respectively, and thus we observe the larger shift at higher fields. We can therefore conclude that the potential operating regime is extended greatly in the nanorod/Tl-2223 composites.

Our results can be compared with those obtained previously in samples containing columnar defects generated by heavy-ion irradiation. In general, the J_c enhancements and the shift of the irreversibility line found in the nanorod/Tl-2223 composites are comparable to those observed in ion-irradiated samples.[6,13] The maximum density of nanorods is, however, lower than the defect density achieved by ion irradiation. Recent improvements in the nanorod density to $>2\times10^{10}$ cm^{-2} and the fact that the true density of correlated defects in the composites is probably greater than the nanorod density due to the formation of misfit dislocations suggest that it will be possible to extend our nanorod approach to high-field applications as well.

In summary, we have shown that MgO nanorods can be used to form composites with Tl-2223 HTS. The nanorods create a well-defined columnar defect structure in the Tl-2223 matrix, and thereby produce significant increases in J_c and a large upward shift in the irreversibility line. These new studies together with previous investigations of nanorod/$Bi_2Sr_2CaCu_2O_z$ composites[9] suggest that our composite approach to creating strong-pinning columnar defects should be broadly applicable to the HTS materials and may be viable for large-scale applications.

This work was supported in part by the Office of Naval Research (N00014-94-1-0302) and the Materials Research Science and Engineering Program of the National Science Foundation (DMR-9400396).

[1] D. Larbalestier, Science **274**, 736 (1996).
[2] J. A. Parell, D. C. Larbalestier, G. N. Riley, Jr., Q. Li, R. D. Parrella, and M. Teplitsky, Appl. Phys. Lett. **69**, 2915 (1996).
[3] D. P. Norton, A. Goyal, J. D. Budai, D. K. Christen, D. M. Kroeger, E. D. Specht, Q. He, B. Saffian, M. Paranthaman, C. E. Klabunde, D. F. Lee, B. C. Sales, and F. A. List, Science **274**, 755 (1996).
[4] D. R. Nelson and V. M. Vinokur, Phys. Rev. Lett. **68**, 2398 (1992).
[5] L. Civale, A. D. Marwick, T. K. Worthington, M. A. Kirk, J. R. Thompson, L. Krusin-Elbaum, Y. Sun, J. R. Clem, and F. Holtzberg, Phys. Rev. Lett. **67**, 648 (1991); P. Kummeth, C. Struller, H. W. Neumuller, and G. Saemann-Ischenko, Appl. Phys. Lett. **65**, 1302 (1994).
[6] R. C. Budhani, M. Suenage, and S. H. Liou, Phys. Rev. Lett. **69**, 3816 (1992).
[7] J. R. Thompson, D. Paul, Z. L. Wang, D. M. Kroeger, and D. K. Christen, Appl. Phys. Lett. **67**, 1007 (1993).
[8] H. Safar, J. H. Cho, S. Fleshler, M. P. Maley, J. O. Willis, J. Y. Coulter, J. L. Ullmann, P. W. Lisowski, G. N. Riley, Jr., M. W. Rupich, J. R. Thompson, and L. Krysin-Elbaum, Appl. Phys. Lett. **67**, 130 (1995).
[9] P. Yang and C. M. Lieber, Science **273**, 1836 (1996).
[10] C. M. Lieber and P. Yang, Patent Pending, Ser. No. #08/606,892.
[11] W. L. Holstein and L. A. Parisi, J. Mater. Res. **11**, 1349 (1996).
[12] C. P. Bean, Rev. Mod. Phys. **36**, 31 (1964).
[13] J. E. Tkaczyk, J. A. Deluca, D. L. Karas, P. J. Bednarczyk, D. K. Christen, C. E. Klabunde, and H. R. Kerchner, Appl. Phys. Lett. **62**, 3031 (1993).